MODEL UNCERTAINTY IN DISCRETE AND SMEARED CRACK PREDICTION IN RC BEAMS UNDER FLEXURAL LOADS

D. Dias-da-Costa[*,1,2], V. Cervenka[3], R. Graça-e-Costa[4,5]

[*]corresponding author (Email: daniel.diasdacosta@sydney.edu.au)

[1]School of Civil Engineering, The University of Sydney, Sydney, NSW 2006, Australia.

[2]ISISE, Department of Civil Engineering, University of Coimbra, Rua Luís Reis Santos, 3030–788 Coimbra, Portugal.

[3]Cervenka Consulting, Na Hrebenkach 55, 15000 Prague 5, Czech Republic.

[4]CEPAC, Universidade do Algarve, Campus de Gambelas, 8005-139 Faro, Portugal.

[5]CEris-ICIST, DECivil, Instituto Superior Técnico, Universidade de Lisboa, Av. Rovisco Pais, 1049-001 Lisboa, Portugal

Abstract

Advanced non-linear finite element models are currently available to perform the design of concrete structures. The development and calibration of the safety factors for the next generation of design guidelines will require a deep understanding of the uncertainty associated with such models. This paper presents a first study focusing on the assessment of the uncertainty of discrete and smeared crack models applied to the simulation of the behavior of RC beams under flexural loads. The discrete strong discontinuity approach (DSDA) and the smeared crack model available in ATENA were chosen for this purpose. Experimental data for mean and maximum crack widths, and average crack spacing for four beams were used as reference. The mesh size dependency and its relation with the uncertainty in the prediction of deflections, crack openings and spacing was investigated. The model uncertainty of mean and maximum crack widths was evaluated for progressive load stages of serviceability conditions for the two crack models considering subsets of data based on the reinforcement ratios and concrete cover.

Keywords: Discrete crack models, smeared crack models, numerical simulation, model uncertainty

Dias-da-Costa, D., Cervenka, V., Graça-e-Costa, R., Model uncertainty in discrete and smeared crack prediction in RC beams under flexural loads, Engineering Fracture Mechanics, Elsevier, 199: 532–543, 2018 (doi: 10.1016/j.engfracmech.2018.06.006).

1. Introduction

Recent advances in material and computational science are widening the capabilities of the finite element method and extending the complexity of structural analyses. Simultaneously, the computational cost of comprehensive simulations is becoming more manageable and this places advanced non-linear models virtually in reach of any designer. Such tools, however, need to properly account for the changes in the structural response caused by fracture. It is well-known that cracking can deeply influence both serviceability conditions and the structural strength of concrete members. At stake is the safety of new and existing structures analysed using computational models.

Many contributions were made in the last decades to the development of crack models for concrete structures. One of the most popular and widely used techniques is based on the smeared crack concept in which the fracture is simulated on an average – i.e. 'smeared' – sense [1-4]. This assumption is particularly convenient for implementation and can easily handle the situations of diffused crack patterns found in concrete structures. However, the true material separation associated with the highly localised cracks cannot be directly simulated. Other limitation includes the 'mesh dependency', where the numerical solution strongly varies with the discretisation [2, 5]. Fortunately, this can be mitigated with specific regularisation techniques [2, 6].

The discrete crack approach can directly deal with the material separation since it mimics the kinematics of the discontinuity [7]. The first attempts found were based on the progressive mesh adaptation with damage propagation [8, 9]. As argued by many authors, this procedure is computationally demanding and can lead to inaccurate mesh representations – e.g. highly distorted elements – without advanced algorithms [10]. Interestingly, elements with high aspect ratio have recently been applied to simulate fracture propagation along the edges of the finite elements with good results – see e.g. [11]. Finite element enrichment approaches can entirely avoid the need for remeshing by applying specific enhancements – e.g. nodal, element or constitutive based – to capture the discontinuous fields associated with the opening of the discontinuity [10, 12-19]. Although the kinematical aspects of the discontinuity are more soundly simulated using a discrete crack approach, the tracking of the propagation of many cracks – particularly in the presence of diffused patterns – can be quite challenging with global formulations. In hybrid approaches, both smeared and discrete techniques are combined, so that the smeared approach is only used to simulate the onset and early stages of fracture propagation. Transition to a discrete crack model is made at the latest stages of damage when the effect of

material separation becomes more relevant [20, 21]. The correct definition of the transition threshold and the connection between formulations are critical aspects for which there is yet no established solution.

2. Research significance

As the advanced computational models become more available, it is no longer enough to validate them using limited experimental data that mostly focus on overall deflections. Instead, a deep technical understanding is now required in ways that are usable by designers and that should cover both ultimate and service limit states. The uncertainty of the advanced non-linear models needs proper quantification, so that reliability analyses [22-26] can be performed to support the development and update of design guidelines, and the proposal of partial safety factors [27-29]. Advanced numerical models often rely on a significant number of parameters, typically many more than standard analytical and classical numerical models, which can become a source for higher uncertainty that needs assessment. Unfortunately, only few numerical studies are available in this regard, and their focus has been mostly centred on ultimate limit states, in which case the prediction of the ultimate load capacity of the concrete structure was aimed [30]. For service limit states, only simplified analytical models for crack widths were deeply studied – see a comprehensive summary in [31]. A numerical study on the ability of a discrete crack approach to predict crack widths for RC beams under flexural loads can be found in [32], although no attempt was made to assess the model uncertainty.

To the best of the authors' knowledge this paper represents the first study on the performance of two crack models in the simulation of RC beams under serviceability. The models are thoroughly assessed in their ability to predict crack widths and spacing based on the model uncertainty supported by experimental data. One approach is based on the smeared crack model and is commercially implemented in software ATENA, whereas the other is a discrete model based on the Discrete Crack Strong Discontinuity Approach (DSDA). More details are provided in the following sections.

3. Model uncertainty concept

Advances in the design assisted by numerical simulations have led to the definition of global safety formats in the *fib* Model Code 2010 [33]. They are based on a probabilistic concept of the involved uncertainties, which can be related to the imperfections in material, geometry and model, among others. It is assumed that the uncertainties are random and can be described by a statistical distribution using its mean and coefficient of

variation. Based on such probabilistic data, which is often obtained with some degree of approximation, the design value of resistance can be calculated for a given reliability level. Since this subject is outside the scope of the paper, the interested reader can find more details in [30, 34, 35]. Similarly to the design situation described for ultimate resistance, the design for serviceability can also be assisted by numerical simulations, in which case the assessment of the crack widths is typically of interest.

The study presented in this paper is devoted to the assessment of the uncertainty of crack models in the scope of serviceability. The model uncertainty reflects the knowledge comprised in the mathematical description of physical cracking and can be referred to as an epistemic uncertainty. Although probabilistic data about model uncertainties is provided in the following sections, the safety formats involved in the serviceability design are not addressed in this publication, as well as the effect of other uncertainties due to material, geometrical and other possible effects. These sources of uncertainties can be treated separately, in a similar way as in the case of resistance. Since the model imperfections are difficult to detect rationally, it is assumed that they are random. Furthermore, despite the assumption of uncertainty decomposition due to its sources, it is evident that the model is affected by material defects, such as non-homogeneities. Thus, the material uncertainty is reduced only to the extent of known basic material parameters, such as tensile strength, fracture energy, among others [25, 36].

The quantification of the model uncertainty in this paper is made using the multiplicative relationship as defined in [25, 36], given by:

$$\theta = \frac{w_{\text{exp}}}{w_{\text{mod}}}, \tag{1}$$

where w_{exp} is the experimental value from the test, and w_{mod} is the value provided by the model. For a series of crack measurements and corresponding simulations, a set of uncertainties θ_i can be generated. By treating the model uncertainty as a random variable, the mean value, μ_θ, and coefficient of variation, V_θ, for the full set of uncertainties can be estimated. The mean value describes the average agreement of the model with the experiment. A mean uncertainty μ_θ, approaching '1' confirms the good agreement, while a deviation from '1' flags a systematic flaw in the model. The coefficient of variation, V_θ, describes the scatter of the model uncertainty and can be used for a probability-based reliability assessment in design.

In this paper, the experimental results from Pérez Caldentey, Peiretti [37] are used to quantify the model uncertainty. Data for mean and maximum crack widths, and average crack spacing in four beams were measured for different load levels, which are herein treated as reference observations of w_{exp}. For the sake of simplicity, the material models are assumed homogeneous with parameters determined from accompanying material tests.

4. Discrete and smeared crack models

The DSDA is selected for the numerical simulations within the scope of the discrete crack approach. A complete description of the method can be found in [15, 38] and only the main features and assumptions are addressed in the following paragraphs.

When adopting the DSDA, it is assumed that the displacement caused by the opening of a discontinuity can be transmitted to its neighbourhood as if it were a rigid body movement. This assumption is reasonable for brittle and quasi-brittle materials, such as concrete, and can be shown to enable addressing the discretisation of discontinuity and neighbouring material as independent. The discontinuity can then be directly embedded within the finite element mesh as if it were an interface element, but without the need to constrain it to the edges of the element. Both discontinuity and continuum contribute to the total displacement at any given point of the body independently, although they remain connected by equilibrium conditions. A set of additional nodes is placed along the path of the crack, such that there is always a node at the intersection points between the crack path and each edges of the element – see Fig. 2. These additional nodes measure the opening of the discontinuity and resulting tractions, which are the quantities of interest for the characterisation of the behaviour of the cracked structure.

During the numerical analysis, new discontinuities are embedded whenever the tensile strength of the material is reached. At the onset of localisation, the discontinuity can still transfer tensile stresses. With the progressive opening of the crack, the stresses are gradually softened until reaching a state of complete separation.

In this paper, the numerical analyses with the DSDA are performed in 2D by assuming plane stress state conditions and using bilinear finite elements. The Rankine criterion is applied to track the onset of localisation and determine the propagation angle, which is then kept fixed upon initiation. As a part of the finite element implementation, only one discontinuity can be embedded in each finite element. New crack paths start from

the centre of the finite element, whereas existing paths propagate from the tip whenever the Rankine criterion is met. The system of equations is solved using the non-iterative automatic procedure proposed in [39]. The reader can find more information about this algorithm and applications to concrete structures in [32, 40-42].

The simulations with the smeared crack model are made using the commercial program ATENA with 2D plane stress representation. During the analysis, the total strains are decomposed into elastic, plastic and fracture parts. The latter component is smeared within the finite elements using a crack band control of strain localisation – see Fig. 2b. The crack band size is related to the element size depending on the crack orientation [43]. The crack orientation is kept fixed during the analysis . It should be mentioned that two modes of failure are considered at the crack face: mode-I due to normal stress and mode-II due to shear stress. More information about the constitutive models can be found in the paper by Cervenka and Papanikolaou [44].

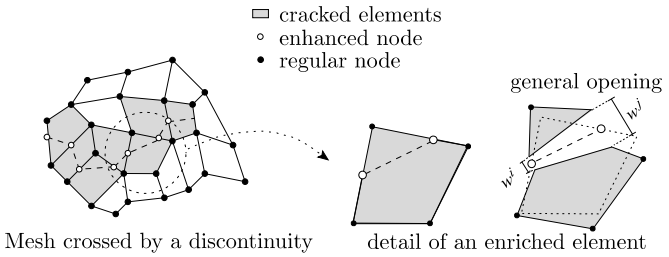

(a)

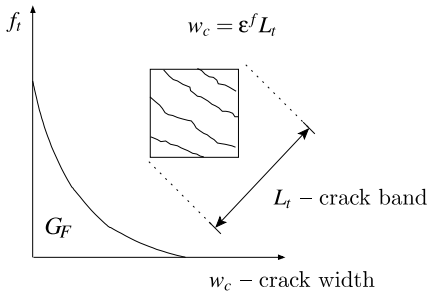

(b)

Figure 1. Crack models: (a) DSDA; (b) smeared approach.

5. Experiments

Results from the experimental programme carried out by Pérez Caldentey, Peiretti [37] are herein used to assess the model uncertainty of the numerical approaches. The selected beam specimens were produced from the same concrete batch and had the geometry and cross-section as represented in Fig. 2. The loading set-up consisted of a four-point bending scheme with a constant moment region over the central span region. A total of four beams – all without stirrups in the central span – and with different combinations of longitudinal reinforcement (four 12 mm steel bars or four 25 mm bars) and concrete cover (20 mm or 70 mm) are herein

chosen for analysis. Each specimen is identified using a generic labelling system ‘d’-‘c’, where ‘d’ stands for the bar diameter and ‘c’ stands for the cover.

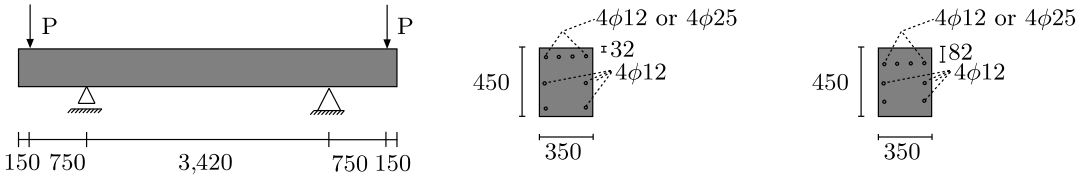

(a) (b) (c)

Figure 2. (a) Set-up; cross-section for specimens: (a) 12-20 and 25-20; and (b) 12-70 and 25-70 (all dimensions in mm).

The experimental study was designed to investigate the process of cracking under increasing flexural loads. The average material properties for concrete were 26.9 MPa and 2.14 MPa, respectively for the compressive and tensile strength, and the steel had a yielding stress of 550 MPa. During the loading, a measurement system registered the displacements for the points located at the mid-span and underneath the applied loads (bottom surface). Longitudinal surface concrete displacements were also measured using DEMECs based on a grid of points 200 mm apart placed at the uppermost edges of the beam. The longitudinal displacements were then used to indirectly determine the crack openings at the top. The crack width was considered given by the displacement between two grid points having into account the number of cracks within the measured length, as discussed and validated by Pérez Caldentey, Peiretti [37]. Having all the openings identified along the mid span of the beam, the average and maximum crack widths could be directly evaluated, as summarised in Table 1. The crack spacing was evaluated for the final stage of loading by inspecting directly the crack pattern of the beam and equating the average distance between consecutive pairs of cracks in the middle span. It should be mentioned that the experimental data is shown at three selected stages of loading roughly corresponding to maximum crack widths of 0.2, 0.4 and 1.0 mm at the level of the main steel reinforcements. As overall observation, for the same rebar diameter the specimens with 70 mm concrete cover have significantly higher average crack spacing and, consequently, also higher crack widths at the same stages of loading. It should be denoted that each crack opening recorded in Table 1 is treated as an independent observation for the model uncertainty in the following sections. This means that each measurement of the crack width is considered not affected by other measurements taken during the test, in which case they can constitute a sample for the calculation of the set of uncertainties, which are independent observations of the model uncertainty – see Eq. (1). These are then used to estimate the average and coefficient of variation for the distribution using standard statistical procedures.

Table 1. Mean and maximal crack width from experiments, Pérez Caldentey, Peiretti [37].

Beam		Stage I	Stage II	Stage III	Av. crack spacing (mm)
12-20	P (kN)	70	90	175	173
	w_{mean} (mm)	0.117	0.198	0.505	
	w_{max} (mm)	0.261	0.396	0.966	
12-70	P (kN)	50	60	100	236
	w_{mean} (mm)	0.192	0.279	0.579	
	w_{max} (mm)	0.328	0.469	1.222	
25-20	P (kN)	100	180	400	131
	w_{mean} (mm)	0.134	0.139	0.346	
	w_{max} (mm)	0.174	0.342	0.834	
25-70	P (kN)	60	100	300	227
	w_{mean} (mm)	0.111	0.205	0.652	
	w_{max} (mm)	0.159	0.356	1.161	

The evaluation of crack widths is based on the following definitions. Average crack width w_{mean} is the average of the crack width values in the investigated span of the beam measured at the top surface for a given load level. The maximum crack width w_{max} is the maximum value found in the span of beam under consideration.

6. Numerical data

The numerical results obtained with the discrete and smeared crack models are herein presented. Only half of the beam (see Fig.1) is modelled by using the appropriate boundary conditions on the axis of symmetry. Two mesh sizes, coarse and fine, see Fig. 3., are used to investigate the impact of the discretisation size on the overall behaviour of the beam and predicted crack patterns.

The steel reinforcements are simulated with linear elements which are connected to the concrete elements using the bond-slip law from Model Code 2010 [33]. Accordingly, the onset of the bond slip is 0.19 MPa and the ultimate peak bond strength is 9.58 MPa for 0.6 mm slip. The Young's modulus for the steel reinforcement is 200 GPa and is linear elastic until yielding; after that, a linear hardening response is followed up to 578 MPa for a strain of 0.1mm/mm. The concrete elements are simulated under plane stress, with a Young's modulus of 30 GPa and a Poisson's ratio of 0.20. Under uniaxial stress, the maximum strength is 26.9 MPa and 2.14 MPa, respectively under compressive and tensile stresses. Cracking is simulated with a mode-I softening model based on the expression proposed by Hordijk [45], with the fracture energy of 0.050 N/mm for a maximum aggregate size of 8 mm, in accordance with the Model Code 1990 [46].

It should be mentioned that the conceptual and practical differences between the smeared and discrete models are found at the discretisation level, i.e., in the representation of fracture within the finite elements, as discussed

in Section 4. Therefore, the constitutive laws and discretisation adopted for concrete, steel reinforcements and bond-slip behaviour described above remain the same for both approaches.

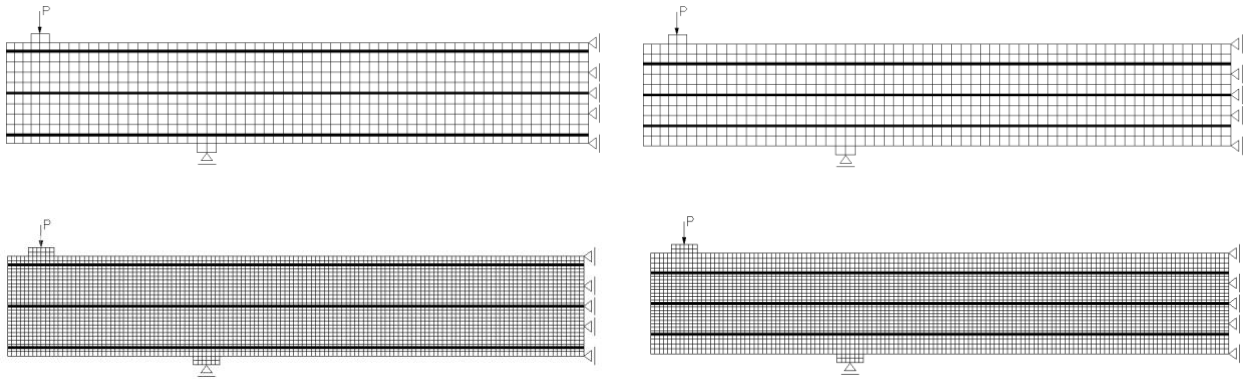

(a) (b)

Figure 3. Coarse and fine meshes adopted for the beams with: (a) 20 mm; and (b) 70 mm cover.

The load vs. displacement curves obtained with both meshes are shown in Fig. 4 for all the beams. As general observation, the coarser mesh can be considered accurate enough for capturing overall deflections, since only negligible differences are identified with increasing discretisation. This also shows that the two approaches are insensitive to the mesh size, at least for displacements.

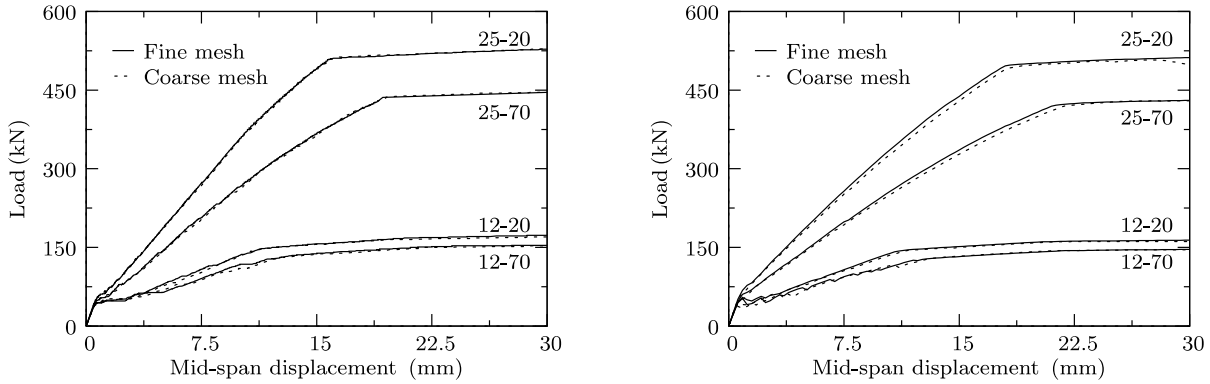

(a) (b)

Figure 4. Load vs. displacement curves: (a) discrete; and (b) smeared models.

Further comparison between models and experimental data, is represented in Fig. 5, where the coarse mesh is used for the simulation. There is a good overall agreement, and both smeared and discrete crack models predict well the typical response stages under increasing flexural load, clearly identifiable by the changes in stiffness associated with the increasing damage. Smeared and discrete models are very similar during the earlier stages of loading and cracking. Differences are only noticed at later stages of loading, where the discrete model provides load capacities slightly above the smeared model for identical vertical displacements.

207 The crack patterns are considered stabilised at the stage III identified in Table 1. Figs. 6 to 9 represent the
208 crack pattern provided by the fine mesh models. In the discrete model, only widths above 0.02 mm are shown
209 magnified 10 times for illustration purposes.

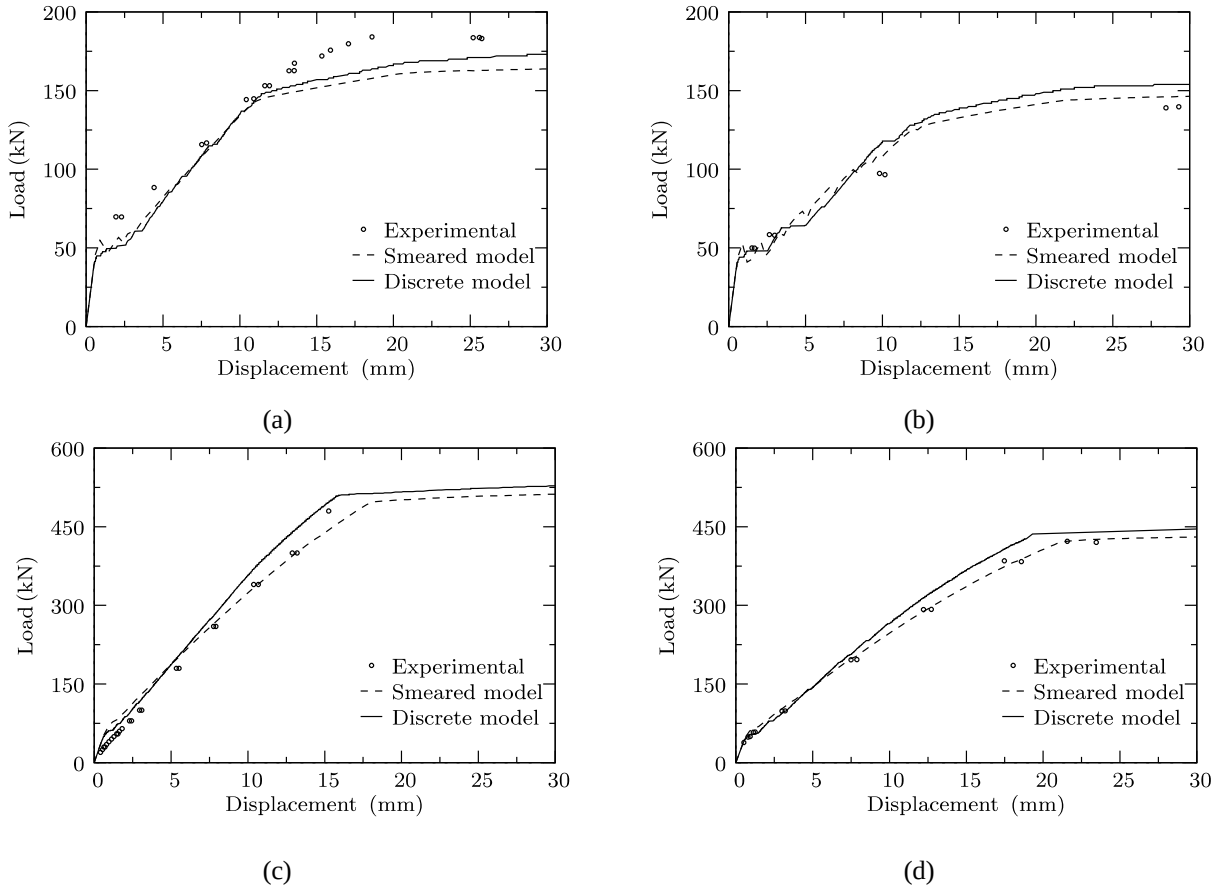

Figure 5. Load vs. displacement curves for specimen (finer mesh): (a) 12-20; (b) 12-70; (c) 25-20; (d) 25-70.

210 Generically, it can be observed that the overall pattern, crack widths and spacing are qualitatively very well
211 predicted by both discrete and smeared approaches. The impact of the concrete cover on the crack width is
212 clearly noticeable in the crack maps, with the number of cracks reducing substantially with its thickness. For
213 the same thickness and load level, the 25 mm bars constrain more effectively the crack propagation along the
214 depth of the beam than the 12 mm bars – compare Figs. 6 and 8.

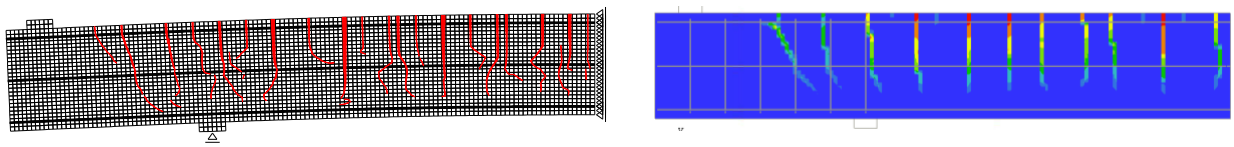

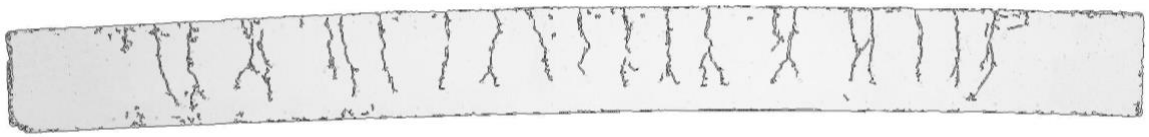

(c)

Figure 6. Crack pattern for specimen 12-20: (a) discrete and (b) smeared model at the third stage of loading; and (c) experimental test at failure.

215

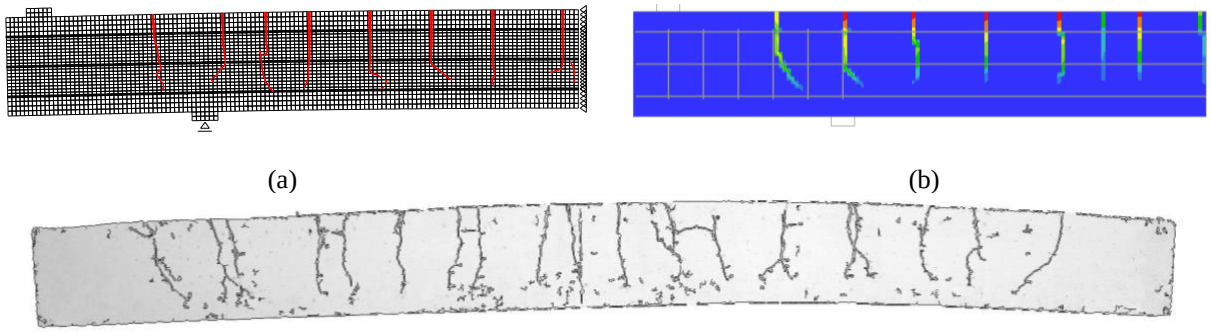

(a) (b)

(c)

Figure 7. Crack pattern for specimen 12-70: (a) discrete and (b) smeared model at the third stage of loading; and (c) experimental test at failure.

216

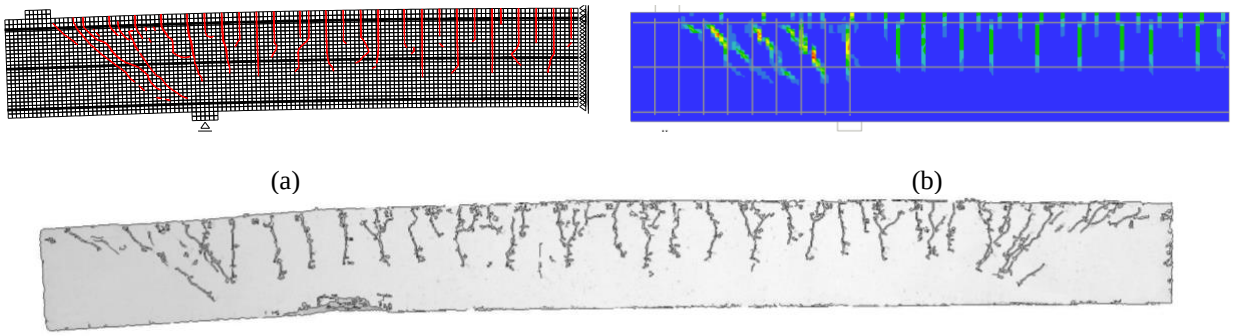

(a) (b)

(c)

Figure 8. Crack pattern for specimen 25-20: (a) discrete and (b) smeared model at the third stage of loading; and (c) experimental test at failure.

217

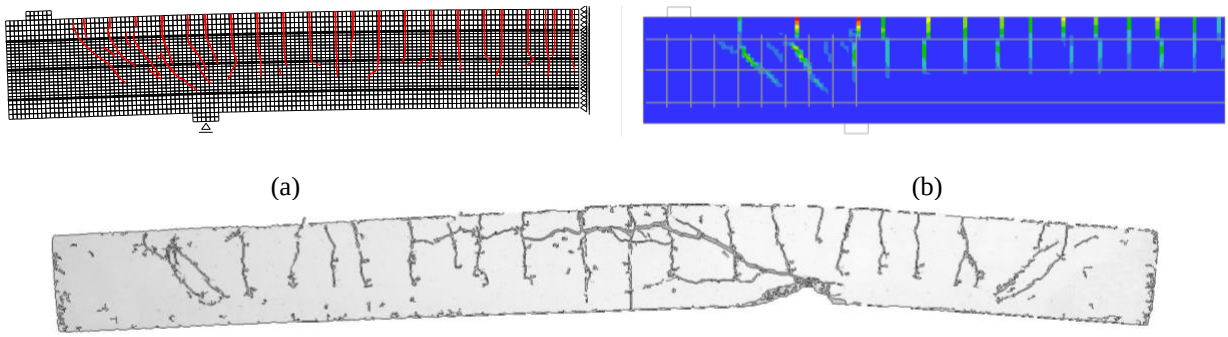

(a) (b)

(c)

Figure 9. Crack pattern for specimen 25-70: (a) discrete and (b) smeared model at the third stage of loading; and (c) experimental test at failure.

Table 2 shows a comparison between experimental and numerical average crack spacing. Numerically, the crack spacing was evaluated by identifying the location of the cracks at the top surface for each model of the beam at the final load stage, and by directly calculating the distance between each consecutive pair of cracks and then the average along the span. In general, the numerical models underestimate the average crack spacing for all the beams tested – except for 12-70. The model uncertainty is above 1.4 for the finer mesh and both approaches. The discretisation has a negligible impact on the discrete model, since the model uncertainty is kept nearly unchanged for each mesh. The smeared crack model provides a better approximation when used with the coarser mesh, in which case the model uncertainty is 1.32.

Table 2. Average crack spacing.

	Exp.	Smeared				Discrete			
Beam	(mm)	Coarse (mm)	θ	Fine (mm)	θ	Coarse (mm)	θ	Fine (mm)	θ
12-20	173	116	1.49	110	1.57	105	1.65	115	1.50
12-70	236	251	0.94	254	0.93	270	0.87	267	0.88
25-20	131	80	1.64	81	1.62	100	1.31	86	1.52
25-70	227	185	1.23	139	1.63	116	1.96	116	1.96
		μ_θ	**1.32**	μ_θ	**1.44**	μ_θ	**1.45**	μ_θ	**1.47**
		V_θ	**0.23**	V_θ	**0.24**	V_θ	**0.32**	V_θ	**0.30**

7. Model uncertainties of crack widths

Tables 3 and 4 summarise all results for average and maximum crack widths, and provide the estimates for the main statistical parameters of the model uncertainty. The overall parameter values are marked in bold. It should be mentioned that the crack openings for the discrete model are obtained directly from the simulations by extracting the opening of each active crack at the top surface of the beam and then computing the average and maximum values in the span. With the smeared model the process is similar after having into account the crack band size – see representation in Fig. 1b.

As a general observation, it can be stated that good predictions are given by both smeared and discrete crack approaches, although the model uncertainty may vary significantly with the formulation and parameter under consideration. The overall model uncertainty for the mean crack width is close to 1.05 using the discrete crack model, a value that denotes the high degree of proximity between prediction and experimental data. The overall variation is also consistent with the values reported for the crack spacing, i.e., less than 0.35. Furthermore, only negligible changes can be identified in the uncertainty parameters with the element size.

The model uncertainty for the smeared approach shows some mesh sensitivity. The best estimates are obtained with the coarse models, situation where the overall uncertainty for the mean crack width is 1.25 and the coefficient of variation 0.45.

Table 3. Uncertainty in the average and maximum crack opening of the discrete model.

	(a) Coarse mesh				Model uncertainty parameters		(b) Fine mesh				Model uncertainty parameters	
					μ_θ	V_θ					μ_θ	V_θ
	P (kN)	70.9	90	159.4			P (kN)	70.1	90.1	160.1		
	w_{mean} (mm)	0.227	0.237	0.4			w_{mean} (mm)	0.239	0.3	0.416		
12-20	w_{max} (mm)	0.284	0.334	0.941			12-20 w_{max} (mm)	0.271	0.366	0.793		
	$\theta_{w\,mean}$	0.515	0.835	1.263	0.87	0.43	$\theta_{w\,mean}$	0.490	0.660	1.214	0.79	0.48
	$\theta_{w\,max}$	0.919	1.186	1.027	1.04	0.13	$\theta_{w\,max}$	0.963	1.082	1.218	1.09	0.12
	P (kN)	50	60	100.2			P (kN)	50	60	100.2		
	w_{mean} (mm)	0.305	0.324	0.52			w_{mean} (mm)	0.252	0.316	0.491		
12-70	w_{max} (mm)	0.31	0.364	0.61			12-70 w_{max} (mm)	0.292	0.368	0.592		
	$\theta_{w\,mean}$	0.630	0.861	1.113	0.87	0.28	$\theta_{w\,mean}$	0.762	0.883	1.179	0.94	0.23
	$\theta_{w\,max}$	1.058	1.288	2.003	1.45	0.34	$\theta_{w\,max}$	1.123	1.274	2.064	1.49	0.34
	P (kN)	99.8	180.5	400.4			P (kN)	100	180.7	400.2		
	w_{mean} (mm)	0.096	0.125	0.273			w_{mean} (mm)	0.116	0.156	0.204		
25-20	w_{max} (mm)	0.13	0.177	0.688			25-20 w_{max} (mm)	0.132	0.213	0.348		
	$\theta_{w\,mean}$	1.396	1.112	1.267	1.26	0.11	$\theta_{w\,mean}$	1.155	0.891	1.696	1.25	0.33
	$\theta_{w\,max}$	1.338	1.932	1.212	1.49	0.26	$\theta_{w\,max}$	1.318	1.606	2.397	1.77	0.31
	P (kN)	59.6	99.9	300.5			P (kN)	60	102	300.8		
	w_{mean} (mm)	0.126	0.165	0.392			w_{mean} (mm)	0.118	0.176	0.405		
25-70	w_{max} (mm)	0.14	0.218	0.561			25-70 w_{max} (mm)	0.13	0.199	0.514		
	$\theta_{w\,mean}$	0.881	1.242	1.663	1.26	0.31	$\theta_{w\,mean}$	0.941	1.165	1.610	1.24	0.28
	$\theta_{w\,max}$	1.136	1.633	2.070	1.61	0.29	$\theta_{w\,max}$	1.223	1.789	2.259	1.76	0.30
All	$\theta_{w\,mean}$	0.855	1.013	1.327	**1.06**	**0.31**	All $\theta_{w\,mean}$	0.837	0.900	1.425	**1.05**	**0.34**
	$\theta_{w\,max}$	1.113	1.510	1.578	**1.40**	**0.29**	$\theta_{w\,max}$	1.157	1.438	1.984	**1.53**	**0.32**

Table 4. Uncertainty in the average and maximum crack opening of the smeared model.

	(a) Coarse mesh				Model uncertainty parameters		(b) Fine mesh				Model uncertainty parameters	
					μ_θ	V_θ					μ_θ	V_θ
	P (kN)	70	90	162			P (kN)	70	90	162		
	w_{mean} (mm)	0.206	0.204	0.937			w_{mean} (mm)	0.187	0.257	0.9		
12-20	w_{max} (mm)	0.245	0.301	1.947			12-20 w_{max} (mm)	0.231	0.31	1.666		
	$\theta_{w\,mean}$	0.568	0.971	0.539	0.69	0.35	$\theta_{w\,mean}$	0.626	0.770	0.561	0.65	0.16
	$\theta_{w\,max}$	1.065	1.316	0.496	0.96	0.44	$\theta_{w\,max}$	1.130	1.277	0.580	1.00	0.37
	P (kN)	50	60	100			P (kN)	50	60	100		
	w_{mean} (mm)	0.237	0.297	0.551			w_{mean} (mm)	0.248	0.279	0.458		
12-70	w_{max} (mm)	0.259	0.345	0.617			12-70 w_{max} (mm)	0.294	0.34	0.611		
	$\theta_{w\,mean}$	0.810	0.939	1.051	0.93	0.13	$\theta_{w\,mean}$	0.774	1.000	1.264	1.01	0.24
	$\theta_{w\,max}$	1.266	1.359	1.981	1.54	0.25	$\theta_{w\,max}$	1.116	1.379	2.000	1.50	0.30
	P (kN)	100	180	400			P (kN)	100	180	400		
	w_{mean} (mm)	0.068	0.094	0.14			w_{mean} (mm)	0.068	0.081	0.198		
25-20	w_{max} (mm)	0.088	0.158	0.412			25-20 w_{max} (mm)	0.088	0.159	0.358		
	$\theta_{w\,mean}$	1.971	1.479	2.471	1.97	0.25	$\theta_{w\,mean}$	1.971	1.716	1.747	1.81	0.08
	$\theta_{w\,max}$	1.977	2.165	2.024	2.06	0.05	$\theta_{w\,max}$	1.977	2.151	2.330	2.15	0.08
	P (kN)	60	100	300			P (kN)	60	100	300		
	w_{mean} (mm)	0.078	0.148	0.511			w_{mean} (mm)	0.059	0.126	0.341		
25-70	w_{max} (mm)	0.091	0.199	0.798			25-70 w_{max} (mm)	0.075	0.17	0.63		
	$\theta_{w\,mean}$	1.423	1.385	1.276	1.36	0.06	$\theta_{w\,mean}$	1.881	1.627	1.912	1.81	0.09
	$\theta_{w\,max}$	1.747	1.789	1.455	1.66	0.11	$\theta_{w\,max}$	2.120	2.094	1.843	2.02	0.08
All	$\theta_{w\,mean}$	1.193	1.193	1.334	**1.24**	**0.45**	All $\theta_{w\,mean}$	1.313	1.278	1.371	**1.32**	**0.41**
	$\theta_{w\,max}$	1.514	1.657	1.489	**1.55**	**0.31**	$\theta_{w\,max}$	1.586	1.725	1.688	**1.67**	**0.33**

Looking at the model uncertainty parameter values individually, it can be concluded that regardless of the crack approach, the model uncertainty for mean crack widths is always smaller or close to 1.0 for the specimens with 12 mm bars – i.e. the lowest reinforcement ratio. The opposite trend is observed in the specimens with 25 mm bars, where the model uncertainty can be significantly above 1. This suggests that both approaches

provide their best estimates for mean crack widths in specimens with smaller reinforcement ratios, situation where the numerical value overestimates the experimental reference. This can be quite relevant for design purposes, as it sets the range where safest estimates can be expected. It also indicates a potential need for model improvement in the case of higher reinforcement ratios.

The highest model uncertainties are found in the maximum crack widths. In this case, the discrete model can underestimate the experimental value by nearly 53% overall, whereas the smeared model underestimates it by 67% with the fine mesh. Both models are also sensitive to the mesh size, but not significantly. Individually, the model uncertainties can be even higher, approaching in some cases the uncertainty value of 2.0. The worst results for this parameter are most likely related with an insufficiency of the modelling assumptions. Indeed, without a random variation of the material properties, the numerical models are unable to capture properly the variations likely to impact on the maximum crack widths. It is speculated that such random material and geometrical defects may be responsible for the underestimation of the maximum crack widths. This observation is quite relevant for design, where quite often good estimates for this parameter are critical. As an additional comment, the experimental measurement of the maximum crack width is also very difficult to obtain and strongly depends on the measurement method. All these factors weigh-in to explain the increased model uncertainty found on maximum crack widths.

The above conclusions are based on limited experimental data including only four independent beam tests. This means that the model uncertainty found is supported by a low confidence. However, the main goal of this study was the comparison of two discretisation methods used for crack propagation in concrete, where the model uncertainty was the tool selected for such comparison. A detailed investigation using more extensive experimental data set would certainly increase the confidence level of the model uncertainty

8. Conclusions

The present study compared two crack models, one based on the discrete crack model and another based on the smeared crack approach. Four reinforced concrete beams tested using a four-point bending scheme were considered as reference. The experimental data included deflections, mean and maximum crack widths and average crack spacing, for three stages of service loads. This data was used to estimate the mean and coefficient of variation for the model uncertainty of the crack widths.

The study in this paper confirmed that the discrete crack model is nearly insensitive to the mesh size not only for displacements, but also for average crack widths and spacing. Good predictions were found for average crack widths, where the average model uncertainty was 1.05 and 1.06, respectively, for the fine and coarse meshes. Such proximity between the two values also further supports the conclusion of mesh independency. The coefficient of variation for the model uncertainty of the discrete approach was nearly the same for the average crack spacing and mean crack widths, with values in the neighbourhood of 0.30.

For the smeared crack model, some mesh sensitivity was found, with the best results provided by the coarse meshes. The mean model uncertainty and corresponding coefficient of variation for average crack widths were, respectively, 1.24 and 0.45. When analysing each model in detail, it was concluded that both smeared and discrete crack approaches have a similar trend in their estimates, with the crack widths being overestimated for the smallest reinforcement ratios and underestimated for the highest ones, although the discrete crack model showed a better performance.

The model uncertainty in the maximum crack widths was very high for both crack models, with values that could reach 2. Such poor estimation could be attributed to the insufficiency of the modelling assumptions, which did not account for imperfections and material defects.

Following this work several recommendations are worth mentioning. In terms of design, the general belief that extremely refined meshes provide better results was not observed, particularly for the smeared crack models. In addition, numerical estimates for maximum crack widths based solely on homogeneous material properties can be quite far from reality. Random distributions of material properties may have to be considered for reducing the model uncertainty if better estimates are indeed required.

Acknowledgments

The first author would like to acknowledge the support from the Australian Research Council through its Discovery Early Career Researcher Award (DE150101703) and ARC Projects (DP140100529 and LP140100591), and from the Faculty of Engineering & Information Technologies, The University of Sydney, under the Faculty Research Cluster Program. Acknowledgment is also extended to FCT (Portuguese Foundation for Science and Technology), through ISISE, under project UID/ECI/04029/2013. The second author would like to acknowledge the support by the Czech Science Foundation under Grant 16-04132S.

304 **References**

305 [1] Bazant ZP, Oh BH. Crack band theory of concrete. Materials and Sructures. 1983;16:155-77.

306 [2] Rots JG. Smeared and discrete representations of localized fracture. International Journal of Fracture.
307 1991;51:45-59.

308 [3] Chong KT, Foster S, Gilbert RI. Time-dependent modelling of RC structures using the cracked membrane
309 model and solidification theory. Computers & Structures. 2008;86:1305-17.

310 [4] Cervenka V. Constitutive Model for Cracked Reinforced Concrete. ACI Journal. 1985;82:877-82.

311 [5] Rots JG. Computational modeling of concrete fracture. Delft, the Netherlands: Delft University of
312 Technology; 1988.

313 [6] Borst Rd, Remmers JJC, Needleman A, Abellan M-A. Discrete vs smeared crack models for concrete
314 fracture: bridging the gap. International Journal for Numerical and Analytical Methods in Geomechanics.
315 2004;28:583-607.

316 [7] Hillerborg A, Modeer M, Petersson PE. Analysis of crack formation and crack growth in concrete by means
317 of fracture mechanics and finite elements. Cement and Concrete Research. 1976;6:773-81.

318 [8] Ingraffea AR, Gerstk WH, Gergely P, Saouma V. Fracture mechanics of bond in reinforced concrete.
319 Journal of Structural Engineering. 1984;110:871-90.

320 [9] Cervenka J, Saouma VE. Numerical evaluation of 3-D SIF for arbitrary finite element meshes. Engineering
321 Fracture Mechanics. 1997;57:541-63.

322 [10] Areias PMA, Dias-da-Costa D, Alfaiate J, Júlio ENBS. Arbitrary bi-dimensional finite strain cohesive
323 crack propagation. Computational Mechanics. 2009;45:61-75.

324 [11] Manzoli OL, Maedo MA, Bitencourt LAG, Jr., Rodrigues EA. On the use of finite elements with a high
325 aspect ratio for modeling cracks in quasi-brittle materials. Engineering Fracture Mechanics. 2016;153:151-70.

326 [12] Duarte CAM, Oden JT. An h-p adaptive method using clouds. Computer Methods in Applied Mechanics
327 and Engineering. 1996;139:237-62.

328 [13] Belytschko T, Black T. Elastic crack growth in finite elements with minimal remeshing. International
329 Journal for Numerical Methods in Engineering. 1999;45:601-20.

330 [14] Duarte CAM, Babuska I, Oden JT. Generalized finite element methods for three-dimensional structural
331 mechanics problems. Computers & Structures. 2000;77:215-32.

[15] Dias-da-Costa D, Alfaiate J, Sluys LJ, Júlio ENBS. A comparative study on the modelling of discontinuous fracture by means of enriched nodal and element techniques and interface elements. International Journal of Fracture. 2010;161:97-119.

[16] Oliver J, Cervera M, Manzoli O. Strong discontinuities and continuum plasticity models: The strong discontinuity approach. International Journal of Plasticity. 1999;15:319-51.

[17] Zhang Y, Zhuang X. Cracking elements: A self-propagating Strong Discontinuity embedded Approach for quasi-brittle fracture. Finite Elements in Analysis and Design. 2018;144:84-100.

[18] Liao F, Huang Z. An extended finite element model for modelling localised fracture of reinforced concrete beams in fire. Computers & Structures. 2015;152:11-26.

[19] Nguyen VP, Nguyen GD, Nguyen CT, Shen L, Dias-da-Costa D, El-Zein A et al. Modelling complex cracks with finite elements: a kinematically enriched constitutive model. International Journal of Fracture. 2017;203:21-39.

[20] Jirásek M, Zimmermann T. Embedded crack model: Part II. Combination with smeared cracks. International Journal for Numerical Methods in Engineering. 2001;50:1291-305.

[21] Seabra MRR, de Sa JMAC, Andrade FXC, Pires FFMA. Continuous-discontinuous formulation for ductile fracture. International Journal of Material Forming. 2011;4:271-81.

[22] Wang L, Wang X, Su H, Lin G. Reliability estimation of fatigue crack growth prediction via limited measured data. International Journal of Mechanical Sciences. 2017;121:44-57.

[23] Wang L, Liang J, Yang Y, Zheng Y. Time-dependent reliability assessment of fatigue crack growth modeling based on perturbation series expansions and interval mathematics. Theoretical and Applied Fracture Mechanics. 2018;95:104-18.

[24] Qiu Z, Wang L. The need for introduction of non-probabilistic interval conceptions into structural analysis and design. Science China Physics, Mechanics & Astronomy. 2016;59:114632.

[25] Sýkora M, Holicky M, Prieto M, Tanner P. Uncertainties in resistance models for sound and corrosion-damaged RC structures according to EN 1992-1-1. Materials and Structures. 2015;48:3415-30.

[26] Holický M, Sýkora M, Barnardo Viljoen C, Mensah KK, Retief J. Model uncertainties in reliability analysis of reinforced concrete structures2013.

[27] Bigaj-van Vliet A, Vrouwenvelder T. Reliability in the performance-based concept of fib Model Code 2010. Structural Concrete. 2013;14:309-19.

[28] Pimentel M, Brühwiler E, Figueiras J. Safety examination of existing concrete structures using the global resistance safety factor concept. Engineering Structures. 2014;70:130-43.

[29] Engen M, Hendriks MAN, Øverli JA, Åldstedt E. Reliability Assessments of Large Reinforced Concrete Structures Using Non-linear Finite Element Analyses: Challenges and Solutions. Cham: Springer International Publishing; 2018. p. 1680-8.

[30] Cervenka V. Reliability-based non-linear analysis according to fib Model Code 2010. Structural Concrete. 2013;14:19-28.

[31] Borosnyói A, Balázs GL. Models for flexural cracking in concrete: the state of the art. Structural Concrete. 2005;6:53-62.

[32] Dias-da-Costa D, N. F. do Carmo R, Graça-e-Costa R. Numerical modeling of concrete beams under serviceability conditions with a discrete crack approach and noniterative solution-finding algorithms. Structural Concrete. 2017;18:225-36.

[33] fib. Model Code for Concrete Structures 2010: Wiley-VCH Verlag GmbH & Co. KGaA; 2013.

[34] Atadero RA, Karbhari VM. Calibration of resistance factors for reliability based design of externally-bonded FRP composites. Composites Part B: Engineering. 2008;39:665-79.

[35] Gayton N, Mohamed A, Sorensen JD, Pendola M, Lemaire M. Calibration methods for reliability-based design codes. Structural Safety. 2004;26:91-121.

[36] JCSS Joint Committee on Structural Safety. Probabilistic Model Code, 12th draft2001.

[37] Pérez Caldentey A, Peiretti H, Iribarren J, Soto A. Cracking of RC members revisited: influence of cover, $\phi/\rho s$, ef and stirrup spacing – an experimental and theoretical study. Structural Concrete. 2013;14:69-78.

[38] Dias-da-Costa D, Alfaiate J, Sluys LJ, Areias P, Júlio ENBS. An embedded formulation with conforming finite elements to capture strong discontinuities. International Journal For Numerical Methods In Engineering. 2013;93:224-44.

[39] Graça-e-Costa R, Alfaiate J, Dias-da-Costa D, Sluys LJ. A non-iterative approach for the modelling of quasi-brittle materials. International Journal of Fracture. 2012;178:281-98.

[40] Dias-da-Costa D, Carmo RNF, Graça-e-Costa R, Valença J, Alfaiate J. Longitudinal reinforcement ratio in lightweight aggregate concrete beams. Eng Struct. 2014;81:219-29.

[41] Graça-e-Costa R, Alfaiate J, Dias-da-Costa D, Neto P, Sluys LJ. Generalisation of non-iterative methods for the modelling of structures under non-proportional loading. International Journal of Fracture. 2013;182:21-38.

[42] Dias-da-Costa D, Graça-e-Costa R, Ranzi G, Smith ST. Assessment of the behaviour of FRP-strengthened RC slabs with a discrete crack model. Journal of Composites for Construction. 2018 (in press).

[43] Cervenka V, Pukl R, Ozbolt J, Eligehausen R. Mesh Sensitivity Effects in Smeared Finite Element Analysis of Concrete Structures. Fracture Mechanics of Concrete Structures (FraMCoS 2), Ed FH Wittmann, AEDIFICATIO Publishers, Freiburg, Germany1995. p. 1387‑96.

[44] Cervenka J, Papanikolaou VK. Three dimensional combined fracture–plastic material model for concrete. International Journal of Plasticity. 2008;24:2192-220.

[45] Hordijk DA. Local approach to fatigue of concrete. Netherlands: TUDelft; 1991.

[46] CEB-fib. Model Code 1990: Comité Euro-International du Béton, Thomas Telford, London; 1993.